THE ASTROPHYSICAL JOURNAL, 521:L79–L82, 1999 August 20
© 1999. The American Astronomical Society. All rights reserved. Printed in U.S.A.

A MEASUREMENT OF THE ANGULAR POWER SPECTRUM OF THE MICROWAVE BACKGROUND MADE FROM THE HIGH CHILEAN ANDES

E. TORBET,[1] M. J. DEVLIN,[2] W. B. DORWART,[1] T. HERBIG,[1] A. D. MILLER,[1] M. R. NOLTA,[1]
L. PAGE,[1] J. PUCHALLA,[2] AND H. T. TRAN[1]

Received 1999 April 30; accepted 1999 June 23; published 1999 July 28

ABSTRACT

We report on a measurement of the angular spectrum of the anisotropy of the microwave sky at 30 and 40 GHz between $l = 50$ and $l = 200$. The data, covering roughly 600 deg^2, support a rise in the angular spectrum to a maximum with $\delta T_l \approx 85$ μK at $l = 200$. We also give a 2 σ upper limit of $\delta T_l < 122$ μK at $l = 432$ at 144 GHz. These results come from the first campaign of the Mobile Anisotropy Telescope on Cerro Toco, Chile. To assist in assessing the site, we present plots of the fluctuations in atmospheric emission at 30 and 144 GHz.

Subject headings: atmospheric effects — cosmic microwave background — cosmology: observations

1. INTRODUCTION

The characterization of the cosmic microwave background (CMB) anisotropy is essential for understanding the process of cosmic structure formation (e.g., Hu et al. 1997). If some of the currently popular models prove correct, the anisotropy may be used to strongly constrain cosmological parameters (Jungman et al. 1995; Bond et al. 1998). Here we report the results from the TOCO97 campaign of the Mobile Anisotropy Telescope (MAT) experiment.

2. INSTRUMENT

The MAT telescope is composed of the QMAP balloon gondola and instrument (Devlin et al. 1998), mounted on the azimuthal bearing of a surplus Nike Ajax military radar trailer.[3] The receiver has five cooled corrugated feed horns, one at the K_a band (31 GHz), two at the Q band (42 GHz), and two at the D band (144 GHz). Each of the K_a- and Q-band horns feed two HEMT-based (high electron mobility transistor) amplifiers (Pospieszalski 1992; Pospieszalski et al. 1994) with one in each polarization. The two D-band horns each feed a single SIS detector (Kerr et al. 1993) with one horn in each polarization. This gives a total of eight radiometry channels in the experiment.[4] A Sumitomo mechanical refrigerator cools the HEMT amplifiers to 35 K and the SIS receivers to 4 K.

The telescope optics are similar to those used for three ground-based observing campaigns in Saskatoon, Saskatchewan (Wollack et al. 1997, hereafter SK). The feeds underilluminate an ambient-temperature 0.85 m off-axis parabolic reflector which in turn underilluminates a computer-controlled 1.8 × 1.2 m resonant chopping flat mirror. The beams are scanned horizontally across the sky in a ≈4.6 Hz sinusoidal pattern. The outputs of the detectors are AC coupled at 0.15 Hz and sampled N_c times during each chopper cycle ($N_c = 80$ for the K_a and Q bands, and $N_c = 320$ for the D band). The telescope is inside an aluminum ground screen which is fixed with respect to the receiver and parabola.

The telescope pointing (Table 1) is established through observations of Jupiter and is monitored with two redundant encoders on both the azimuth bearing and the chopper. The absolute errors in azimuth and elevation are 0.°04, and the relative errors are less than 0.°01.

The chopper position is sampled 80 times per chop. When its rms position over one cycle deviates by more than 0.°015 from the average position (due to wind, etc.), we reject the data.

3. OBSERVATIONS AND CALIBRATION

Data were taken at a 5200 m site[5] on the side of Cerro Toco (latitude = −22.°95, longitude = 67.°775), near San Pedro de Atacama, Chile, from 1997 October 20 to 1997 December 15. The receiver was operational 90% of the available time. For the anisotropy data, the primary optical axis is fixed at azimuth = 204.°9, elevation = 40.°5, $\delta = -62.°6$, and the chopper scans with an azimuthal amplitude of 2.°96 (8.°93 on the sky) as the sky rotates through the beam. The telescope position was not wobbled to the other side of the south celestial pole as for the SK measurements in the north. The rms outputs of the K_a2 and $D1$ channels are shown in Figure 1.

Jupiter is used to calibrate all channels and map the beams. Its brightness temperature is 152, 160, and 170 K for the K_a through D bands, respectively (Griffin et al. 1986; Ulich et al. 1981), with an intrinsic calibration error of ≈5%. We account for the variation in angular diameter. We also observe Jupiter with multiple relative azimuthal offsets to verify the chopper calibration.

The uncertainty in the beam solid angle for the K_a and Q bands is ≈5% as determined from the standard deviation of beam measurements for the MAT and QMAP experiments. From a global fit of the clear-weather Jupiter calibrations, the standard deviation in the fitted amplitudes is 6%. These sources of calibration error dominate the error from the uncertainty in the passband. The total 1 σ calibration error is obtained by

[1] Princeton University, Physics Department, Jadwin Hall, Princeton, NJ 08544.
[2] University of Pennsylvania, Department of Physics and Astronomy, David Rittenhouse Laboratory, Philadelphia, PA 19104.

[3] Details of the experiment, synthesis vectors, data, and analysis code may be found at http://www.hep.upenn.edu/CBR and http://physics.princeton.edu/~cmb.

[4] HEMT amplifiers have improved considerably since this time (Pospieszalski et al. 1997) and SIS receivers are generally more sensitive than what we achieved. In 1997, one of the D channels and one of the Q channels did not have sufficient sensitivity to warrant a full analysis.

[5] The Cerro Toco site of the Universidad Católica de Chile was made available through the generosity of Professor Hernán Quintana, Department of Astronomy and Astrophysics. It is near the proposed Millimeter Array (MMA) site.

TABLE 1
TOCO97 Beam Characteristics

Feed	Azimuth (deg)	Elevation (deg)	$\Omega_{\rm meas}$ (10^{-4} sr)	$\theta_{\rm avg}^{\rm FWHM}$ (deg)
$K_a1/2$	203.13	41.75	2.75	0.90
$Q1/2$	206.75	41.85	1.69	0.70
$Q3/4$	206.70	39.25	1.77	0.72
$D1$	205.00	40.44	0.183	0.23

combining the intrinsic, beam, and measurement errors in quadrature resulting in 10%, 10%, and 11% in K_a through D, respectively.

A thermally stabilized noise source at $T_{\rm eff} \approx 1$ K is switched on twice for 40 ms every 100 s as a relative calibration. The pulse height is correlated to the Jupiter calibrations in the K_a and Q channels. The variation in detector gain corrected for with these calibration pulses is roughly 5%. No such correction was made for the D band.

4. DATA REDUCTION

The data reduction is similar to that of the SK experiment (Netterfield et al. 1997). The raw data, d_i, are multiplied by "n-point" synthesis vectors, $\mathrm{SV}_{n,i}$ (where i ranges from 1 to N_c), to yield the effective temperature corresponding to a multilobed beam on the sky, $H(\Omega)$. For example, we refer to the classic three-lobed beam produced by a "double difference" as the "three-point harmonic" and write $t_3 = \sum_{i=1}^{N_c} \mathrm{SV}_{3,i} d_i$. We also generate the quadrature signal q_n (data with chopper sweeping in one direction minus that with the sweeping in the other direction) and fast-dither signal f_n^d (one value of t_n minus the subsequent one). For both $K_a1/2$ and $Q3/4$ we analyze the unpolarized weighted mean of the combined detector outputs.

The phase of the data relative to the beam position is determined with both Jupiter and observations of the galaxy. We know we are properly phased when the quadrature signal from the galaxy is zero for all harmonics.

The harmonics are binned according to the right ascension at the center of the chopper sweep. The number of bins depends on the band and harmonic (Table 2). For each night, we compute the mean and variance of all the t_n, q_n, and f_n^d corresponding to a bin. These numbers are appropriately averaged over the campaign and used in the likelihood analysis.

From the raw data set of 814,250 5 s averages, we filter out time spent on instrument calibration (6%), celestial calibrations (11%), observations of the galaxy and daytime (53%), and bad pointing (4%). Accounting for overlap, these cut a total of 57%. The data span R.A. = 0°–140° ($b = -55°$ to $-10°$).

The data are selected according to the weather by examining each harmonic independently. We first flag 5 s averages with a large rms. The unflagged data are divided up into 15 minute sections and the rms of the t_n found. For 15 minute sections with rms greater than 2 σ, the constituent 5 s averages are not used, as well as those of the preceding and succeeding 15 minute sections. We ensure that the cut does not bias the statistical weight. As a final cut, nights with less than 4.7 hr of data are excluded. Repeating the analysis with increased cut values produces statistically similar (within 1 σ) results. The atmosphere cut selects roughly the same sections for K_a and Q. In the analyses, we discard the two- and three-point data as they are corrupted by atmospheric fluctuations and variable instrumental offsets. If the four-point data are corrupted, it is at the 1 σ level and not readily detectable.

The stability of the instrument is assessed through internal consistency checks and with the distribution of the offset of each harmonic. The offset is the average of a night of data after the cuts have been applied (ranges from 5 to 10 hr) and is of magnitude $\approx$200 μK with error 20 μK. In general, the offset remains constant for a few nights and then jumps 3–5 σ. The resulting χ^2/ν is typically between 4 and 20 for the data over the full campaign and is $\approx$1 for the quadrature signal. In general, a change in offset can have any timescale. The q_n and f_n^d are sensitive to $\tau = 0.25$ s. We also monitor a slow dither (difference of the subsequent 5 s averages) with $\tau = 5$ s and a night-to-night dither with $\tau = 24$ hr. For the final analysis, we delete one 7 day section that has a large jump in offset. To eliminate the potential effect of slow variations in offset, we remove the slope and mean for each night. This is accounted for in the quoted result (both the constraint matrix method [Bond et al. 1998b] and marginalization [Bond et al. 1991] give similar corrections) and does not significantly alter the results over the subtraction of a simple mean. As a test, we have also tried removing quadratic and cubic terms from the offset, with no significant changes in the answer. In summary, there is no evidence that the small instability in the offset affects our results.

We examined the variations in the power spectrum of the synchronously co-added raw HEMT data and found no evidence for microphonics. However, a microphonic coupling to the SIS detector was exacerbated after situating the telescope at the site. After filtering, residual signals persisted in the quadrature channels (although not in the fast and slow dithers), and so we report only 95% upper limits for the D channel, specifically $\delta T_l < 180$ μK at $l = 325$ and $\delta T_l < 122$ μK at $l = 432$.

The primary effect of data editing is to increase the error bar per point and decrease the upper limits of the null tests. Of the 169 null tests (Table 2 plus fast, slow, and night dithers),

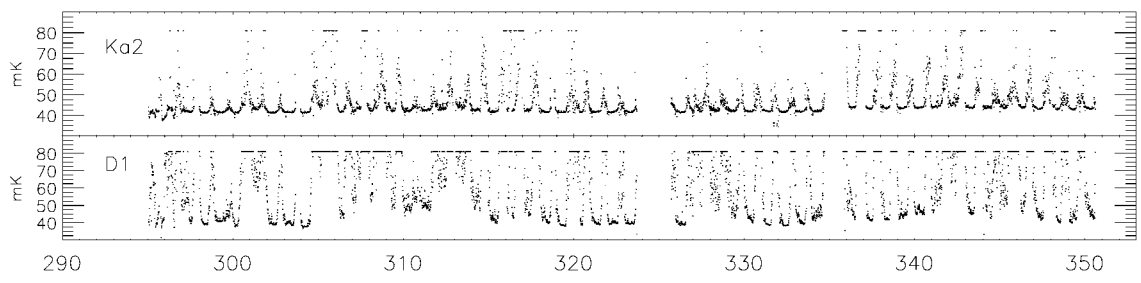

Fig. 1.—The rms detector output in antenna temperature of the K_a2 and $D1$ channels averaged over 0.68 ms (with the chopper running at the nominal amplitude) vs. day of year in 1997. The sky is most stable between 10 P.M. and 10 A.M. local time. Similar results from 1998 are consistent with the NRAO opacity measurements (see http://www.tuc.nrao.edu/mma/sites/sites.html).

TABLE 2
TOCO97 ANGULAR SPECTRUM

Band and SV	$l_{\rm eff}$ [a]	δT_l [b] (μK)	$N_{\rm bins}$ [c]	$\delta T_l'$ (μK)	$\Delta_{\rm tot}$ (μK)	$\Delta_{\rm inst}$ (μK)	$[I(W)]^{1/2}$	$(A-B)/2$ [d,e] (μK)	Quad, q_n [d] (μK)	$(H1-H2)/2$ [d,f] (μK)
K_a1/2:										
4 point	63^{+17}_{-18}	35^{+13}_{-9}	48(16)	32	33	20	0.84	<27(0.94)	<30(1.05)	<29(0.95)
5 point	86^{+16}_{-21}	52^{+11}_{-8}	64(28)	49	40	21	0.71	<21(0.59)	<32(1.23)	<29(1.05)
6 point	107^{+16}_{-21}	71^{+12}_{-10}	96(42)	69	52	27	0.65	<32(0.90)	<31(0.96)	<35(1.04)
7 point	127^{+16}_{-22}	93^{+15}_{-14}	96(41)	90	57	27	0.55	<35(0.80)	<37(0.90)	<30(0.68)
8 point	145^{+18}_{-20}	103^{+15}_{-13}	128(55)	102	63	34	0.52	<51(0.97)	<46(1.00)	<43(0.91)
9 point	165^{+18}_{-20}	65^{+16}_{-17}	128(54)	59	47	38	0.46	<63(0.95)	<72(1.19)	<66(1.07)
10 point	182^{+21}_{-17}	67^{+20}_{-23}	192(82)	70	60	51	0.44	<68(0.85)	<69(0.94)	<60(0.89)
11 point	192^{+30}_{-8}	<119	192(82)	67	65	58	0.42	<91(0.94)	<83(1.00)	<86(0.96)
12 point	215^{+27}_{-11}	128^{+30}_{-33}	192(82)	127	83	68	0.37	<150(1.11)	<86(0.79)	<76(0.67)
$Q$1:										
4 point	63^{+17}_{-18}	57^{+18}_{-13}	48(20)	51	53	31	0.83	...	<44(1.04)	<47(1.11)
5 point	87^{+16}_{-22}	40^{+14}_{-14}	64(28)	34	40	33	0.71	...	<36(0.75)	<47(1.09)
6 point	110^{+15}_{-24}	56^{+14}_{-13}	96(42)	52	52	40	0.65	...	<45(0.87)	52^{+15}_{-14}(1.71)
7 point	131^{+14}_{-25}	81^{+19}_{-16}	96(42)	77	59	41	0.55	...	<65(1.12)	<53(0.89)
8 point	151^{+15}_{-25}	86^{+19}_{-17}	128(55)	79	66	50	0.53	...	<45(0.67)	<64(0.89)
9 point	172^{+14}_{-26}	93^{+23}_{-23}	128(55)	89	68	54	0.47	...	<82(0.94)	<72(0.83)
10 point	191^{+16}_{-24}	<115	192(84)	31	75	74	0.47	...	<105(1.13)	<92(0.94)
11 point	203^{+24}_{-17}	<117	192(84)	44	80	78	0.44	...	<103(0.94)	<83(0.81)
12 point	221^{+25}_{-15}	<169	192(84)	91	91	84	0.40	...	<138(1.06)	<119(0.92)
13 point	245^{+21}_{-20}	<130	192(84)	...	84	92	0.37	...	<163(1.02)	<164(1.06)
14 point	267^{+20}_{-23}	<202	256(112)	123	123	114	0.37	...	<183(1.06)	<188(1.00)
$Q$3/4:										
5 point	83^{+15}_{-20}	47^{+17}_{-13}	64(17)	43	39	24	0.73	31^{+10}_{-8}(1.94)	<50(1.39)	<58(1.73)
6 point	106^{+14}_{-23}	61^{+18}_{-13}	96(22)	55	46	28	0.66	<27(0.68)	<34(0.60)	<61(1.46)
7 point	125^{+14}_{-23}	72^{+16}_{-12}	96(35)	71	50	30	0.56	<29(0.65)	<57(1.30)	<31(0.57)
8 point	145^{+14}_{-23}	115^{+19}_{-15}	128(45)	109	68	35	0.54	<26(0.50)	<38(0.73)	<60(1.18)
9 point	165^{+14}_{-24}	72^{+24}_{-21}	128(29)	65	48	37	0.48	<43(0.82)	<97(1.38)	<84(1.16)
10 point	184^{+15}_{-23}	87^{+19}_{-19}	192(70)	86	63	48	0.47	<68(1.03)	<45(0.78)	<52(0.75)
11 point	196^{+22}_{-17}	90^{+27}_{-26}	192(54)	84	65	53	0.44	<64(0.90)	<78(0.91)	<75(0.78)
12 point	212^{+25}_{-13}	100^{+29}_{-27}	192(65)	97	69	57	0.40	<70(0.95)	<129(1.36)	<84(0.89)
13 point	236^{+20}_{-19}	< 157	192(56)	80	71	65	0.37	<107(1.07)	<121(0.93)	<153(1.17)
14 point	258^{+18}_{-23}	119^{+36}_{-38}	256(103)	119	91	80	0.36	<116(0.95)	<137(1.11)	<103(0.78)

NOTE.—A "<" indicates a 95% confidence limit. Calibration errors are *not* included.

[a] The range for $l_{\rm eff}$ denotes the range for which the window function exceeds $e^{-1/2}$ times the peak value.

[b] The error on $\delta T_l = [l(l+1)C_l/2\pi]^{1/2}$ is composed of experimental uncertainty and sample variance. These values are not statistically independent: harmonic numbers differing by 2 are correlated at the 0.35 level. For all harmonics, the square root of the sample variance $[\propto 1/(2N_{\rm bins})^{1/2}]$ is ≈ 7 μK.

[c] The number of bins on the sky followed by, in parentheses, the number used in the analysis due to the galactic/atmosphere cut.

[d] The reduced χ^2 are given in parentheses. The standard deviation on $\chi^2\nu$ is $\approx(2/[N_{\rm bins}^{-2}])^{1/2}$.

[e] $(A-B)/2$ is the difference in polarizations. We have combined bands and harmonics to generate 95% upper limits on polarization, $A-B$, and obtain $(l,\ \delta T_l\ [\mu{\rm K}]) = (63^{+18}_{-18},\ <37)$, $(86^{+17}_{-21},\ <54)$, $(115^{+21}_{-24},\ <28)$, $(148^{+17}_{-25},\ <41)$, $(195^{+33}_{-23},\ <79)$.

[f] $(H1-H2)/2$ is the first half minus the second half.

there are only three failures. The distribution of the reduced χ^2 of the null tests is consistent with noise and inconsistent with any signal. When the data are combined into groups of harmonics and bands, all null tests are consistent with noise.

5. ANALYSIS AND DISCUSSION

The analysis of the individual harmonics, because the windows are so narrow, essentially corresponds to finding $\delta T_l' = [(\Delta_{\rm tot}^2 - \Delta_{\rm inst}^2)/I(W)]^{1/2}$, where $\Delta_{\rm tot}^2$ is the variance of the data for each harmonic, $\Delta_{\rm inst}^2$ is the variance due to atmospheric and instrumental noise, and $I(W) = \sum W_l/l$. The term W_l is the window function, as defined in Bond (1996). The full likelihood analysis provides a formal way of determining δT_l that includes correlations and gives the correct error bar in the low signal-to-noise limit.

The error in $I(W)$ is determined from the scatter in the beam values. We find $\delta I(W)/I(W) \lesssim 0.01$ for all bands and harmonics. The mean variance $\Delta_{\rm inst}^2$ is determined directly from the uncertainties in each bin. If these uncertainties are somehow biased, the results of the simple test and full likelihood will be biased. We examine the distribution of all the data for each harmonic from all the nights after removing the mean value of each sky bin. The width of this distribution agrees with the mean error bar, indicating that the error per point is not biased. Also, the ratio of the error bars between harmonics agrees with the analytic calculation.

In the full analysis (Fig. 2), we include all known correlations inherent in the observing strategy. From the data, we determine the correlations between harmonics due to the atmosphere, detector noise, and nonorthogonality of the synthesis vectors. The correlation coefficients between bands due to the atmosphere are of order 0.05. We also examine the autocorrelation function of the data for a single harmonic to ensure that atmospheric fluctuations do not correlate one bin to the next. The quoted results are insensitive to the precise values of the off-diagonal terms of the covariance matrix.

These results are similar to previous results obtained with this technique (SK), although the experiment was done with different optics, a different receiver, a different primary calibrator, largely different analysis code, and observed a different part of the sky. Although we have not correlated our data with templates of foreground emission, the foreground contribution is known to be small at these frequencies and Galactic latitudes (Coble et al. 1999; de Oliveira-Costa et al. 1997). In addition,

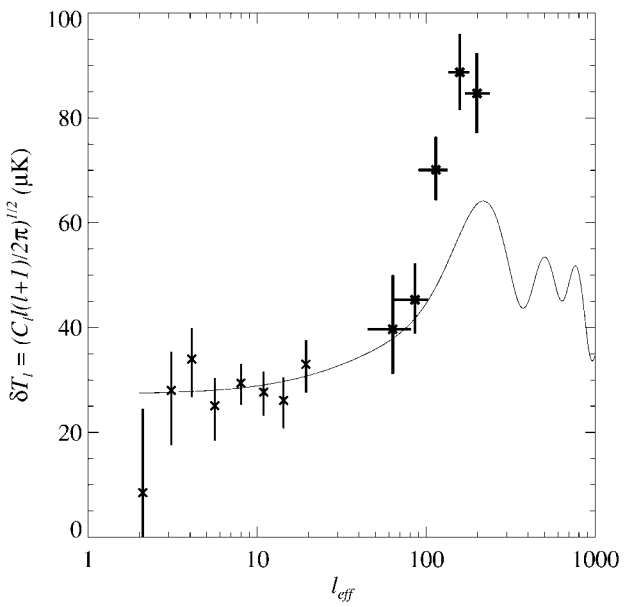

FIG. 2.—Combined analysis of data in Table 2. The values are $(l, \delta T_l\ [\mu\mathrm{K}]) = (63^{+18}_{-18}, 40^{+10}_{-9})$, $(86^{+16}_{-22}, 45^{+7}_{-6})$, $(114^{+20}_{-24}, 70^{+6}_{-6})$, $(158^{+22}_{-23}, 89^{+7}_{-7})$, $(199^{+38}_{-29}, 85^{+8}_{-8})$. Error bars are "1 σ statistical"; calibration error is not included. The *COBE*/DMR points are from Tegmark (1997). The solid curve is standard CDM ($\Omega_b = 0.05$, $h = 0.5$).

we have examined the frequency spectrum of the fluctuations in the K_a and Q bands and find it to be consistent with a thermal CMB spectrum and inconsistent with various foregrounds. Finally, the full analysis has been repeated after deleting each 15° section of data in right ascension, indicating that the signal does not arise from one region. (Our scan passes near, but misses, the Large Magellanic Cloud.) Future work will address the precise level of contamination.

We gratefully acknowledge the insights and help from Dave Wilkinson, Norm Jarosik, Ray Blundell, Angel Otárola, Hernán Quintana, Robert Caldwell, Ted Griffith, Bernard Jones, and Harvey Chapman. The experiment would not have been possible without NRAO's site monitoring and detector development. We also thank Lucent Technologies for donating the radar trailer. This work was supported by an NSF NYI award, a Cottrell Award from the Research Corporation, a Robert H. Dicke Fellowship to E. T., a David and Lucile Packard Fellowship (to L. P.), a NASA GSRP fellowship to A. M., an NSF graduate fellowship to M. N., NSF grants PHY 92-22952, PHY 96-00015, AST 97-32960, and the University of Pennsylvania. The data will be made public upon publication of this Letter.

REFERENCES

Bond, J. R. 1996, Theory and Observations of the Cosmic Microwave Background Radiation, in Cosmology and Large-Scale Structure (Les Houches Session LX, 1993 August), ed. R. Schaeffer, J. Silk, M. Spiro, & J. Zinn-Justin (Amsterdam: Elsevier), 469
Bond, J. R., Efstathiou, G., Lubin, P. M., & Meinhold, P. R. 1991, Phys. Rev. Lett., 66, 2179
Bond, J. R., Efstathiou, G., & Tegmark, M. 1998, MNRAS, 50, L33
Bond, J. R., Jaffe, A. H., & Knox, L. 1998, Phys. Rev. D, 57, 2117
Coble, K., et al. 1999, preprint (astro-ph/9902195)
de Oliveira-Costa, A., Kogut, A., Devlin, M. J., Netterfield, C. B., Page, L. A., & Wollack, E. J. 1997, ApJ, 482, L17
Devlin, M. J., de Oliveira-Costa, A., Herbig, T., Miller, A. D., Netterfield, C. B., Page, L., & Tegmark, M. 1998, ApJ, 509, L73
Griffin, M. J., Ade, A. R., Orton, G. S., Robson, E. I., Gear, W. K., Nolt, I. G., & Radostitz, J. V. 1986, Icarus, 65, 244
Hu, W., Sugiyama, N., & Silk, J. 1997, Nature, 386, 37
Jungman, G., Kamionkowski, M., Kosowsky, A., & Spergel, D. N. 1995, Phys. Rev. D, 54, 1332
Kerr, A. R., Pan, S.-K., Lichtenberger, A. W., & Lloyd, F. L. 1993, in Proc. Fourth Int. Symp. on Space Terahertz Technology, 1993 March 30–April 1, Los Angeles, 1
Netterfield, C. B., Devlin, M. J., Jarosik, N., Page, L., & Wollack, E. J. 1997, ApJ, 474, 47
Pospieszalski, M. W. 1992, IEEE MTT-S Digest, 1369
———. 1997, in Microwave Background Anisotropies, ed. F. R. Bouchet et al. (Gif-sur-Yvette: Editions Frontières), 23
Pospieszalski, M. W., et al. 1994, IEEE MTT-S Digest, 1345
Tegmark, M. 1997, Phys. Rev. D, 55, 5895
Ulich, B. L. 1981, AJ, 86, 1619
Wollack, E. J., Devlin, M. J., Jarosik, N., Netterfield, C. B., Page, L., & Wilkinson, D. 1997, ApJ, 476, 440 (SK)